

# IRIS PHASE III NUMERICAL SIMULATIONS OF IMPACT INDUCED VIBRATIONS OF REINFORCED CONCRETE STRUCTURE UNDER MISSILE IMPACT

Genadijs Sagals<sup>1</sup>, Nebojsa Orbovic<sup>1</sup> and Christopher Cole<sup>2</sup>

<sup>1</sup>Technical Specialist, Canadian Nuclear Safety Commission, Ottawa, ON, Canada

<sup>2</sup>Director, Canadian Nuclear Safety Commission, Ottawa, ON, Canada

## ABSTRACT

This paper describes the work conducted by the Canadian Nuclear Safety Commission (CNSC) related to the numerical simulations of reinforced concrete (RC) structure under deformable missile impact. This work was conducted as part of the OECD/NEA IRIS (Improving Robustness Assessment Methodologies for Structures Impacted by Missiles) Phase 3 benchmark project. The paper presents the simulation results of tests conducted at VTT Technical Research Centre in Espoo, Finland. The current paper is a continuation of the work conducted by the authors for Phases 1 and 2 of the IRIS project. The main objective of Phase 3 is to model the transmission of the induced vibrations through a reinforced concrete structure from the impacted wall to the floors and walls of the structure which are outside the impacted area. The simulation results are subsequently compared with the test data.

A special mock-up was build and tested at the VTT test facility. The test results were made available for all participants in the IRIS Phase 3 benchmarking exercise which included 29 teams from 18 different countries. The parameters of the missile and RC structure were selected to ensure a flexible behaviour of the RC target in the impact area with only moderate damages: specifically cracking and permanent deformation without perforation. The non-linear dynamic behaviour of the reinforced concrete slabs under missile impact was analysed using the commercial Finite Element (FE) code LS-DYNA. Both solid and shell FE models were employed for the target discretization. As the ultimate objective of this work is to model the entire structure over long time periods, several simplified models were developed for the RC target. These include full shell and combined shell-solid models with distributed (smeared) and explicitly defined reinforcement. Multiple suitable concrete models from LS-DYNA library were selected for analysis to account for the loading condition. The FE predictions are generally in reasonable agreement with test results, showing similar target displacements for all sensor locations.

## 1. INTRODUCTION

Modern Canadian and International design codes and regulatory documents for Nuclear Power Plants require design against impact of externally or internally generated missiles on concrete safety related structures. This requirement stimulated a large amount of analytical and experimental work conducted in different countries. The most noticeable tests were conducted in Germany (so called Meppen Impact Tests, Nachtsheim and Stangenberg (1981)), the full scale test at Sandia (Sugano et al. (1993) and in Finland (Impact I-III tests conducted by VTT Technical Research Centre, Vepsä et al. (2011)). Based on publicly available data from these tests, two simulation workshops IRIS\_2010 and IRIS\_2012 were conducted; see Berthaud et al. (2011), Vepsä et al. (2011) and Orbovic et al. (2015). The authors of the current paper also actively participated in both workshops and developed an adequate FE model (Sagals et al. (2011) and Orbovic, Sagals et al. (2015)) that is capable of predicting the main characteristics of post-impact state of a concrete slab, such as perforation velocity, size and shape of damaged area, crack patterns, etc.

However, the impact-induced vibrations were not addressed in previous studies. No tests were also conducted so far to examine impact induced vibrations and their propagation through a reinforced concrete structure. Therefore, it was decided to conduct the new International simulation workshop IRIS Phase 3 in the framework of the OECD/NEA, with the main objective of Phase 3 to analyse the transmission of the impact induced vibrations through a reinforced concrete structure from the impacted wall to the floors and walls of the structure which are outside the impacted area. The workshop has two distinctive stages as follows:

- At the first stage a special mock-up and the hollow deformable missile were manufactured and tested at the VTT test facility, see Figs. 1 and 2. The parameters of the missile and RC structure were selected to ensure a flexible behaviour of the RC target in the impact area with only moderate damages: specifically cracking and permanent deformation without perforation. The test results were made available for all workshop participants to compare simulation results with the test data and make the necessary adjustments and calibrations of their models. The description and preliminary analysis of this mock-up were provided in Schneeberger et al. (2014).
- At the second stage another mock-up with different shape and additional attached structures imitating equipment was build and tested at the VTT test facility. To assess the cumulative damage three subsequent impacts with different missile velocities were conducted for the second test. Contrary to the first test, the second test results were not provided to workshop participants in order to allow for “blind” simulations. After submitting modelling results to Organizing Committee, test results will be released and conclusion made.

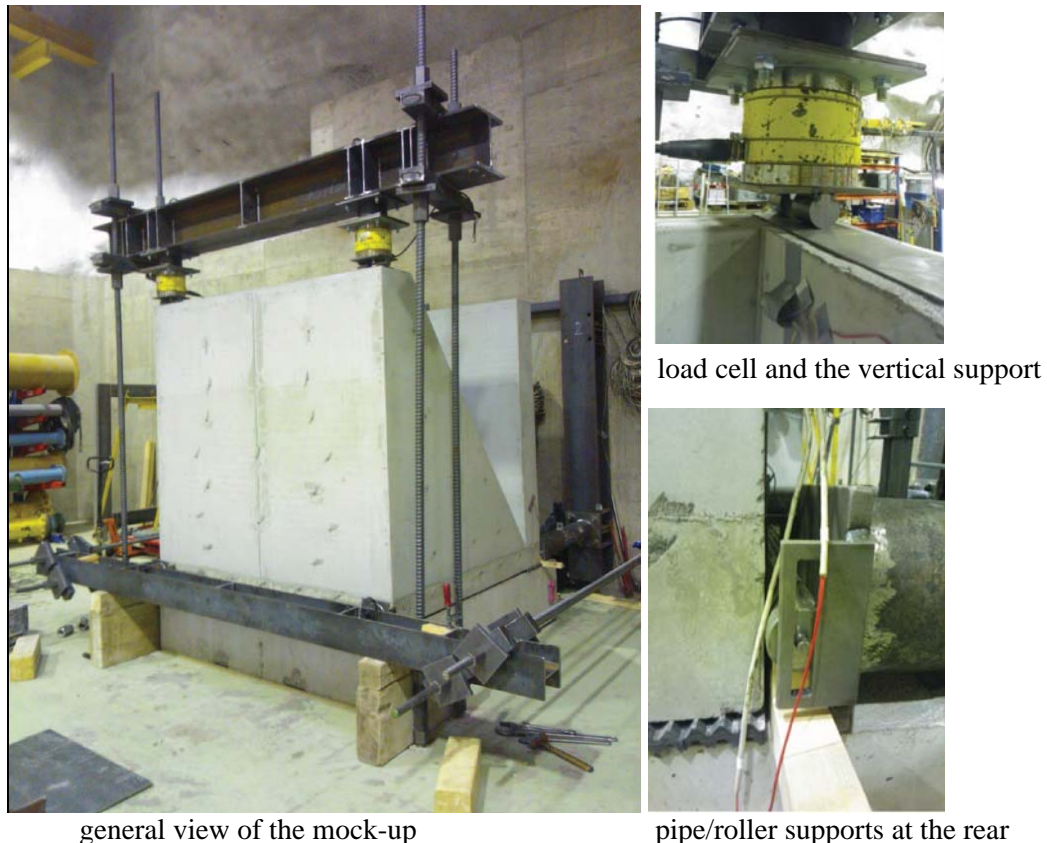


Figure 1. Concrete mock-up for the first stage

## The missile

Impact speed: 113.7 m/s  
Hit point 38 mm to the right and 37 mm  
above the centre of the front wall

- Soft (empty stainless steel) missile
- Steel grade EN1.4432
- $\Phi=254$  mm,  $t=2$ mm
- $L=2311$  mm
- Realized mass 50.1 kg

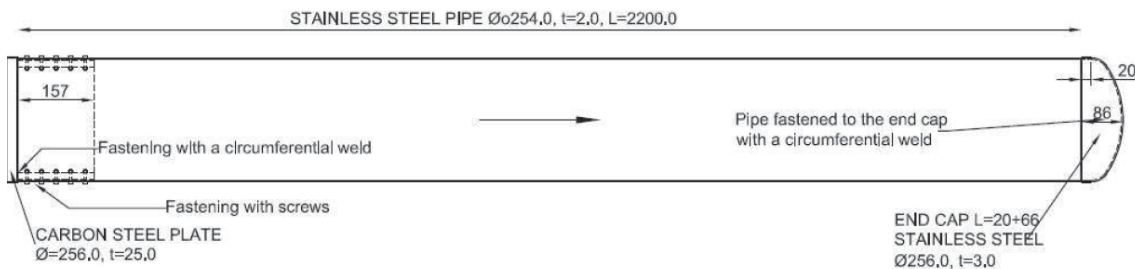


Figure 2. The missile

Since the current paper is written before the second test results were provided, only modelling of the first test is presented.

## 2. FE MODELING

As mentioned in the previous section, the authors have earlier developed FE model that was successfully used for modelling of the missile impact on the reinforced concrete slab. This model is based on commercial explicit code LS-DYNA (LS-DYNA R8.0 User's Manual). However, this model includes fine 3-D mesh with solid FE and explicit modelling of reinforcement. Using this type of FE model for a structure consisting of several slabs and for much longer simulation time to capture impact induced vibrations leads to very large modelling time. Additionally, authors believe that this approach is impractical for real large structures, such as nuclear containment building.

However, the test runs conducted show that a simplified shell model of the mock-up does not produce adequate results as described in section 3.1 below. Therefore, a new simplified hybrid model was developed to simulate mock-up behaviour. This model consists of solid FE around the impact zone and shell FE for the rest of the mock-up and the missile. The detailed description of this new model is provided below in sections 2.1 – 2.3.

### 2.1 FE Mesh

Fig. 3 shows the new hybrid solid/shell model developed. Due to symmetry, only  $\frac{1}{2}$  of the entire model with appropriate symmetry BC at  $x=0$  plane was employed in analysis. Belytschko-Tsay 4-noded shell elements (default shell FE in LS-DYNA) were used for modeling of the shell part of the mock-up and the missile. The solid 3-D part of the front wall around the impact area was modeled using 3-D constant stress solid 8-noded elements (also default solid FE in LS-DYNA). FE density was selected based on test runs as described in section 3.1 below.

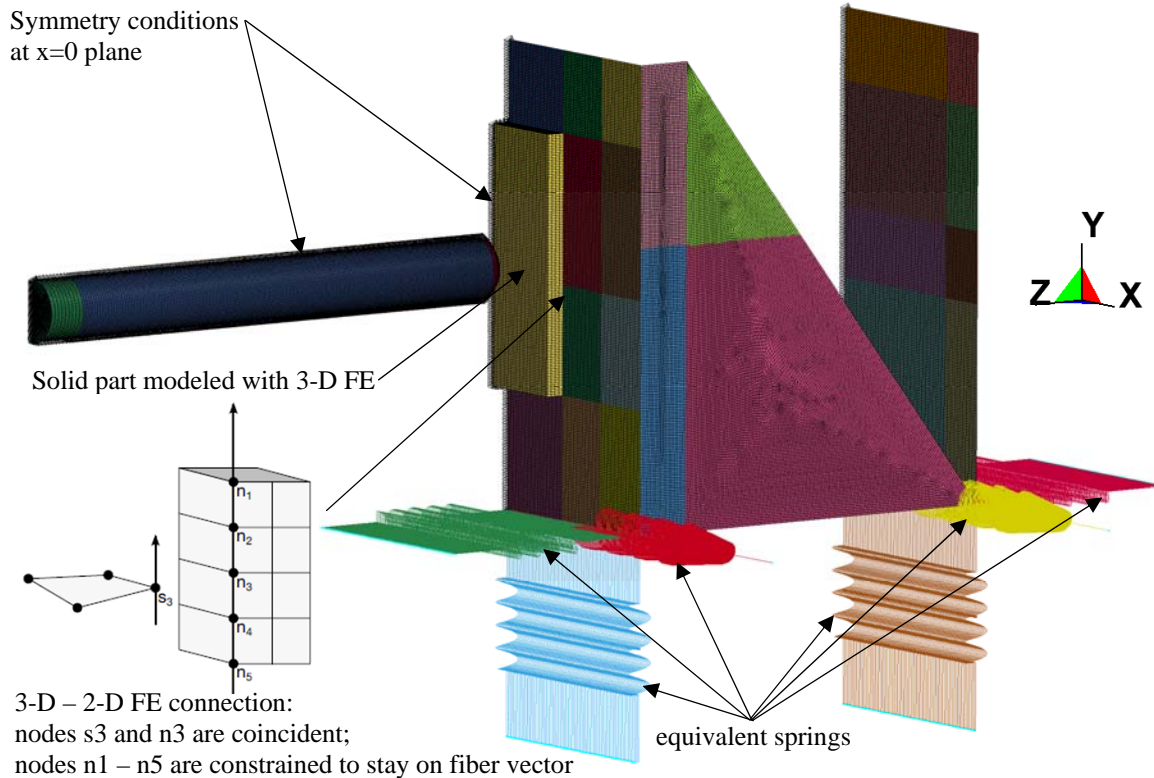


Figure 3. Hybrid solid/shell FE model

The connection between solid and shell FE was modeled using `CONSTRAINED_SHELL_TO_SOLID` command (LS-DYNA R8.0 User's Manual) that align brick nodes lying along the tangent vector to the nodal fiber, see Fig. 3.

## 2.2 Material modeling and parameters

### Concrete:

Unfortunately, the same concrete material models cannot be used in LS-DYNA for both shell and solid parts. Therefore, based on previous successful experience, solid part with 3-D FE (front wall around impact) was modeled using material model #84 (\*MAT\_WINFRITH\_CONCRETE without strain-rate) and the following parameters:

$E=24.55\text{GPa}$ ,  $\rho=2207\text{kg/m}^3$ ,  $\nu=0.17$ ,  $\text{UTC}= 50.9\text{MPa}$  (cubic),  $\text{UTS}= 2.63\text{MPa}$ , aggregate size=8mm ( $\emptyset$ ), and default pressure versus volumetric strain curve.

Shell parts were modeled using material model #172 (\*MAT\_CONCRETE\_EC2). Material data and equations governing the behavior of this model are taken from Eurocode 2 Part 1.2 (General rules – Structural fire design), hereafter referred to as EC2 with the following parameters:

Walls:

$\rho=2207\text{kg/m}^3$ ,  $\text{UTC}= 47.2\text{MPa}$  (cylinder),  $\text{UTS}= 2.63\text{MPa}$

Floor:

$\rho=2198\text{kg/m}^3$ ,  $\text{UTC}= 53.7\text{MPa}$  (cylinder),  $\text{UTS}= 3.42\text{MPa}$

Default values were selected for other remaining concrete parameters.

### Reinforcement for solid FE:

Smear (distributed through FE) reinforcement was used in both shell and solid 3-D parts of the FE model. Fraction of reinforcement in each direction was calculated as ratio of reinforcement to concrete areas in that direction. Shear (transverse) reinforcement was not accounted for in shell parts. The material properties were selected as follows:

3-D FE:

$E=200$  GPa,  $\sigma_y=619$  MPa ( $\varnothing 6$  mm wall),  $E_t=694$  MPa, ultimate elongation 12.27%

2-D FE:

$E=200$  GPa,  $\nu=0.3$ ,  $\sigma_u=707.4$  MPa ( $\varnothing 6$  mm floor), 603.9 MPa ( $\varnothing 10$  mm floor), 695.6 MPa ( $\varnothing 12$  mm floor), 703.8 MPa ( $\varnothing 6$  mm wall), 636 MPa ( $\varnothing 8$  mm wall) and 665.5 MPa ( $\varnothing 10$  mm wall).

Default values were selected for other remaining reinforcement parameters.

### Missile:

The material properties were selected as follows:

$E=200$  GPa,  $\nu=0.3$ ,  $\sigma_y=350$  MPa,  $\sigma_u=633$  MPa,  $E_t=623.3$  MPa, fracture strain 45.4%.

Cowper-Symonds strain rate model was selected:  $C=100$  1/s,  $p=10$ .

### Damping:

Explicit FEA does not have inherent numerical damping. Therefore, additional mass and stiffness weighted damping was employed in FE model. The damping values were selected based on typical values and on comparison with test results as follows:

Mass weighted damping:

3-D part: mass damping 5% of critical (corresponding frequency  $f=f_3=85$  Hz);

2-D parts: mass damping 3% of critical (corresponding frequency  $f=f_2=23.8$  Hz); where  $f_2$  and  $f_3$  are the 2<sup>nd</sup> and 3<sup>rd</sup> modal frequencies calculated in separate FEA and representing first significant bending modes for the rear and front walls correspondingly.

No Stiffness weighted damping was applied for both missile and mock-up.

### 2.3 Boundary conditions modeling

Bi-trapez® bearings (see Fig. 1) were employed to support the bottom of mock-up. They were modeled as elastic springs with equivalent stiffness in all 3 directions attached to each correspondent FE node, see Fig.3. Another spring node was fixed for all springs. The equivalent stiffness in each direction was calculated based on manufacturer datasheet ([www.calenberg-ingenieure.com](http://www.calenberg-ingenieure.com)). Front, back and top supports were provided using steel rollers to simplify BC for modeling (see Fig. 1). Roller-mock-up contact was modeled as nodes (roller) to surface (mock-up) contact.

## 3. MODELING RESULTS

Modeling results were arranged into two groups as follows: (i) comparison between different FE models to establish adequate model and mesh density, and (ii) compare FE predictions for selected output variables with test results.

### 3.1 Comparison between different FE models

As was mentioned earlier in section 2, the use of detailed 3-D solid FE model for the entire mock-up is impractical. However, the fully 3-D solid and fully shell models were created and compared to ensure that shell model could adequately transfer impact induced vibrations from the impact zone to the rest of the system and, specifically, to the back wall. Since the 3-D and 2-D FE have different concrete material models, elastic concrete model with typical properties was selected for this comparison to exclude effect of different concrete models. The results show that the difference in displacements for shell and solid models is not significant for the nodes at the centre of the back wall and above. However, the results show a significant difference for the relatively much smaller displacement of the bottom nodes of the back wall.

The next comparison was conducted for the following two cases:

- Fully shell model versus hybrid solid/shell model described in section 2.1
- Explicit reinforcement using beam FE versus smeared reinforcement.

Concrete material models, test boundary conditions and missile impact loading were applied in these cases. Horizontal and vertical displacements of the front and back panels and reaction forces were selected for comparison. The modelling results show that:

- Hybrid mock-up model produced better results (closer to test results) comparing with fully shell model, particularly in impact zone, and
- The mesh size of approximately 10 mm (approximately 200 FE across the entire mock-up width in x-direction) and, additionally, 8 FE through the thickness for the solid part of the model) is adequate for modeling mock-up behavior. For the deformable steel missile the mesh size of approximately 4.5 mm for missile head and part of the side shell close to the head and 11 mm for the rest of the missile is adequate. Missile deformations and force transfer to the mock-up during impact and rebound were considered.

### 3.2 FE predictions and test results

In this section FE predictions were combined in several groups and compared with test results where possible. Due to large number of output parameters and test recordings we will focus on the FE predictions where the reliable test results exist to provide comparison.

#### Missile results

Fig. 4 shows deformed shape and shortening of the missile after impact. The results clearly show similarity between FE predictions and test results. However, the total predicted length of the deformed missile is longer than test value.



Figure 4. Deformed shape of the missile after impact

Next Fig. 5 shows FE predictions for time histories of missile z-velocity calculated at the back end of the pipe and missile impulse. The predicted missile rebound velocity is ~5m/s. Unfortunately, no test result exists for this value.

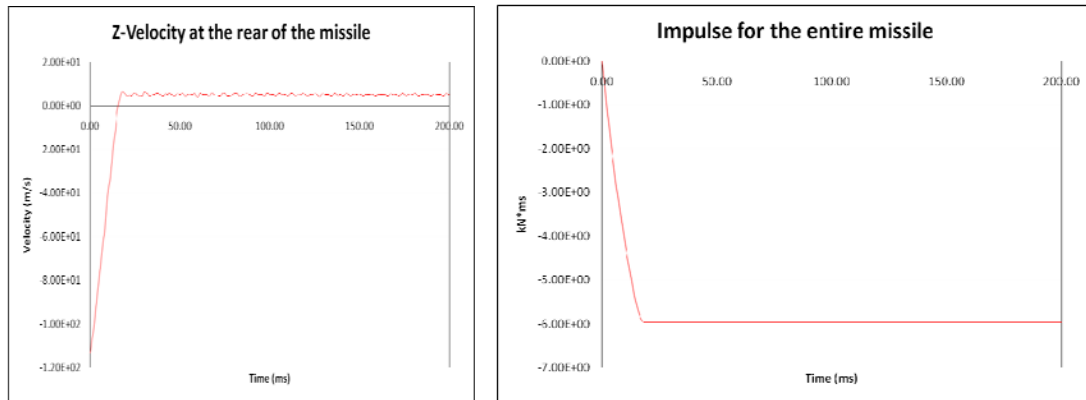


Figure 5. Missile FE predictions

### Mock-up results

For mock-up the global damage, displacements, accelerations and support forces were calculated and compared with test results when possible. Reinforcement was not explicitly modeled. Therefore, reinforcement strains cannot be obtained for the 3-D (Winfrith) concrete FE. While shell EC2 concrete FE provide some reinforcement strain values, the authors were not confident how and where they were calculated. Therefore, reinforcement strains are not discussed in this paper. From all test results for mock-up the recorded displacements are the most reliable. Therefore, due to a limited size of the paper, we will focus on mock-up displacements only. Fig. 6 shows sensors locations on the mock-up together with maximum, minimum and residual values of recorded displacements. Next Fig.7 shows both predicted and measured displacements at sensors D1-D3.

The results show higher predicted maximum displacements of the front wall during the impact (sensor D1). Together with larger predicted length of the deformed missile this is, probably, an indication of higher missile strain-rate hardening during the impact. Unfortunately, test results are not sufficient to identify the proper value of strain-rate hardening for both missile and concrete.

Test results also show significantly higher vibrations decay at sensor D1 location due to damping. The attempts to match this decay in FE modeling resulted in unreasonably high damping coefficients for the system. However, the accurate modeling of the structure behavior in the impact zone is not the objective of the simplified model developed. More accurate models are required for this modeling as described earlier in sections 1 and 2.

Good agreement is obtained for the console wall displacement (sensor D2). The predicted minimum and maximum values are -9/+11.06 mm. They are in a good agreement with the measurements (-10.14/+8.59 mm). Good agreement is also obtained for vibrations decay at this location due to damping. This means that FE model adequately transfer impact loading to the back console panel thus meeting the main objective of this work.

Not so good agreement is obtained for the vertical displacement at the rear bottom location (sensor D3). The predicted minimum and maximum values for the sensor D3 are -8.66/+5.63 mm. They are significantly higher than the measurements (-2.46/+2.55 mm). The reason is, probably, some friction in contact between mock-up and frame. Shell approximation also could play a role since the sensor location cannot be adequately identified in the shell model.

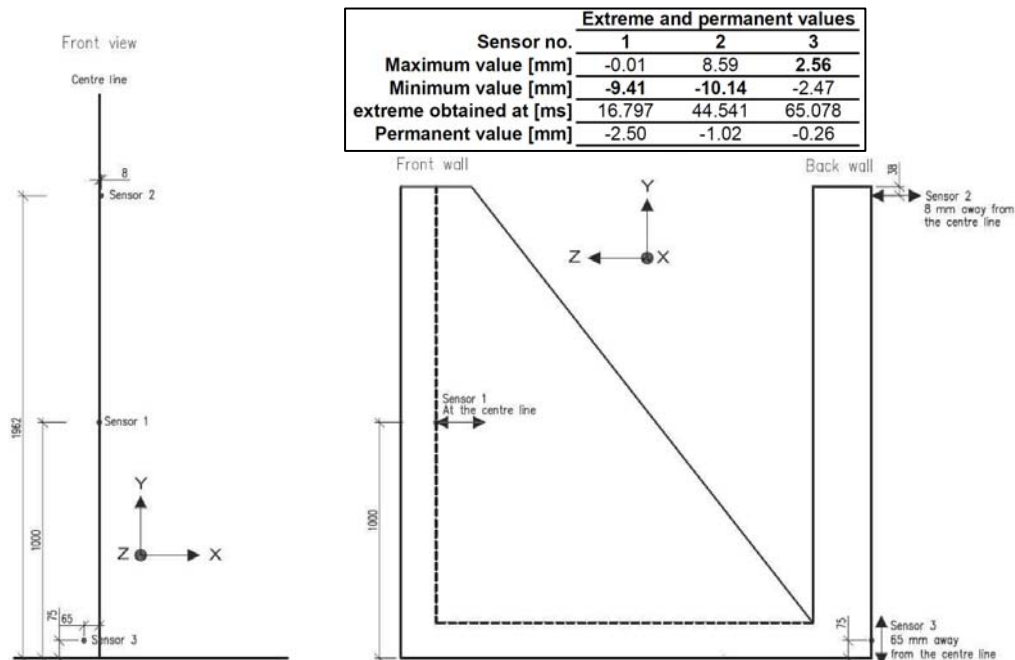


Figure 13. Displacement sensors locations on the mock-up

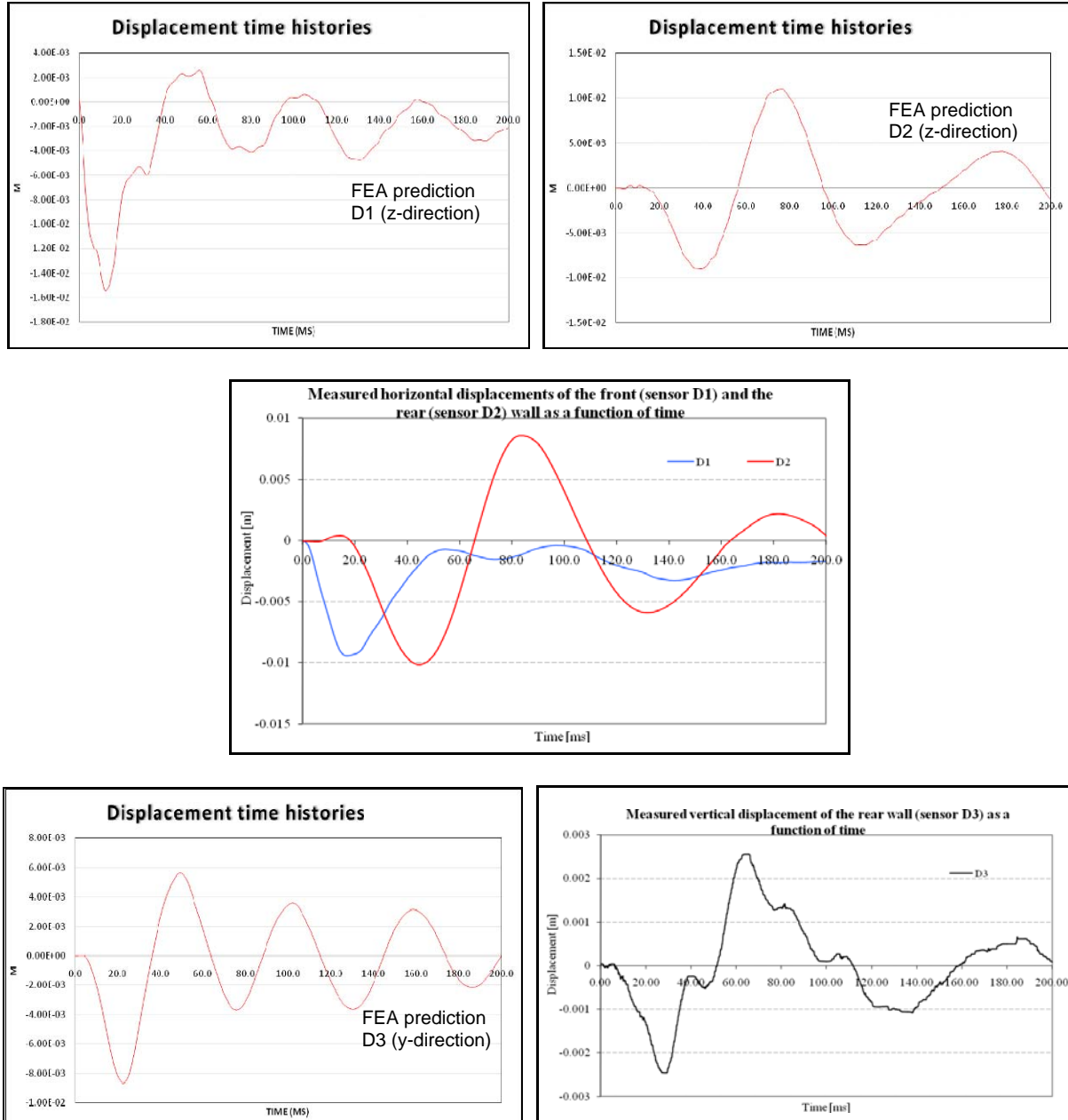


Figure 7. Predicted and measured displacements at sensors D1, D2 and D3

Finally, Fig. 8 shows mock-up damage after the missile impact. Damage is displayed based on capabilities of selected FE. For 3-D solid FE (Winfrith concrete model) cracks are shown explicitly. For the shell FE (EC2 concrete model) number of cracks inside each FE (0, 1 or 2) is presented.

The results show some cracks on the front and side panels. On the back cantilever panel some cracks are evident on the bottom part only (at the roller-wall contact). I should be kept in mind that both concrete models show all possible cracks, even very small cracks that are practically invisible. Therefore, the real number of visible cracks will be smaller than shown in Fig.8. For the 3-D part (Winfrith concrete model) it is possible to select only cracks that are larger than some size. Fig. 9 shows cracks larger than 0.1mm in this part.

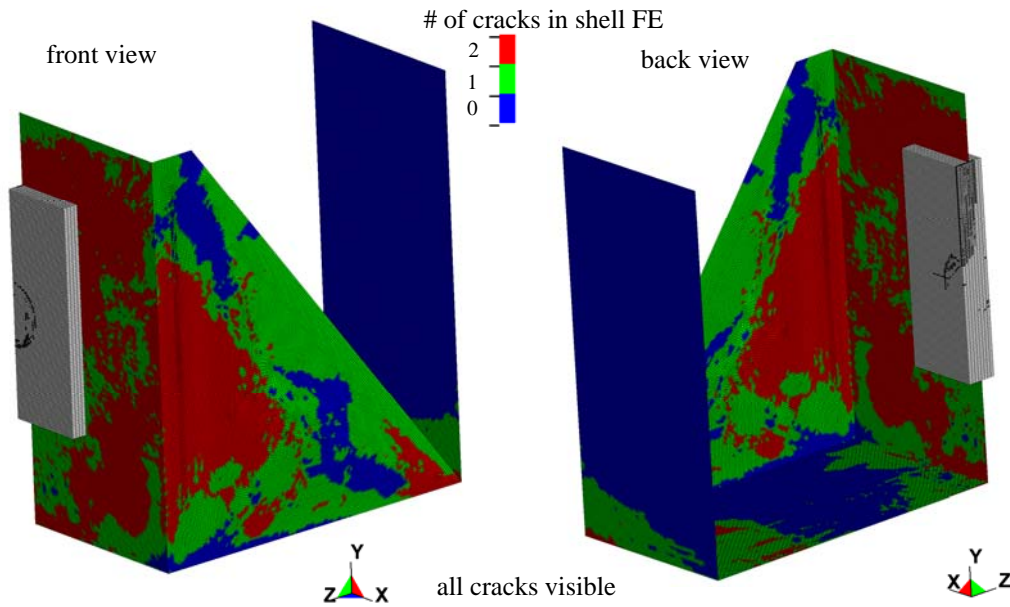


Fig. 8 Mock-up damage after missile impact.

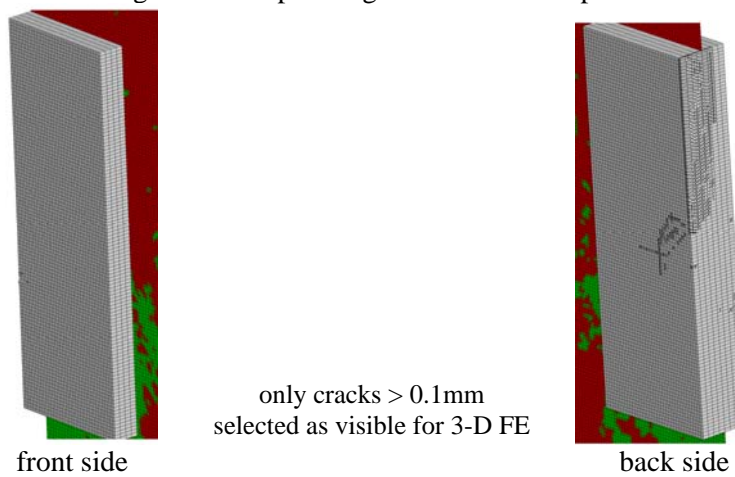


Fig. 9 Mock-up damage after missile impact.

#### 4. CONCLUSIONS

FE model developed provides satisfactory results for mock-up and missile deformations. The results clearly show similarity between FE predictions and test results for the deformed missile. The predicted “folded” part of the missile is 174 mm versus 180 mm measured. However, the total predicted length of the deformed missile is longer than test value (1250 mm versus 1085 mm measured).

The predicted maximum displacement at sensor D1 (back side of the front wall at the impact location) is higher than measured (15.39mm versus 9.37mm measured). The possible reasons of this discrepancy are:

- The simplified modeling of reinforcement as smeared inside concrete FE
- Reinforcement strain-rate hardening could not be included
- Using shell FE instead of solid
- Unknown strain-rate law and parameters for the deformable missile and concrete
- Unknown friction value at missile-target contact

The results also show significantly higher vibrations decay in the test at sensor D1 location. The attempts to match this decay in FE modeling resulted in unreasonably high damping coefficients for the system. However, the accurate modeling of the structure behavior in impact zone was not the objective of the simplified model developed.

Good agreement is obtained for the console wall displacement (sensor D2). The predicted minimum and maximum values are -9/+11.06 mm. They are in a good agreement with the measurements (-10.14/+8.59 mm). Good agreement is also obtained for vibrations decay at this location due to damping. This means that FE model adequately transfer impact loading to the back console panel thus meeting the main objective of this work.

Time histories provided show that the real system damping is more complex than simplified linear mass/stiffness weighted damping used in the current FE model.

Not so good agreement was obtained for the vertical displacement at the rear bottom location (sensor D3). The predicted minimum and maximum values for the sensor D3 are -8.66/+5.63 mm. They are significantly higher than the measurements (-2.46/+2.55 mm). The reason is, probably, some friction in contact between mock-up and frame. Shell approximation also could play a role since the sensor location cannot be adequately identified in the shell model.

## REFERENCES:

- Berthaud Y., Benboudjema F., Colliat J.-B., Tarallo F., Orbovic N., Rambach J.-M. (2011). "IRIS\_2010 - PART IV: NUMERICAL SIMULATIONS OF FLEXURAL VTT-IRSN TESTS," *Transactions of the SMiRT 21*, 6-11 November, New Delhi, India, pp 855-862.
- Calenberg Ingenieure. "bi-Trapez Bearing®," <http://www.calenberg-ingenieure.com>
- LS-DYNA® R8.0 User's Manual. (2015), LIVERMORE SOFTWARE TECHNOLOGY CORP. (LSTC).
- Nachtsheim W., Stangenberg F. (1981). "Impact of deformable missiles on reinforced concrete plates-comparisational calculations of Meppen tests," *Transactions of the 6<sup>th</sup> SMiRT*, Paris, France.
- Orbovic N., Tarallo F., Rambach J.-M., Sagals G. and Blahoianu A. (2015). "IRIS\_2012 OECD/NEA/CSNI benchmark: Numerical simulations of structural impact", *Nuclear Engineering and Design*, 295, 700–715.
- Orbovic N., Sagals G. and Blahoianu A. (2015). "Influence of transverse reinforcement on perforation resistance of reinforced concrete slabs under hard missile impact," *Nuclear Eng. and Design*, 295, 716–729.
- Sagals G., Orbovic N. and Blahoianu A. (2011). "SENSITIVITY STUDIES OF REINFORCED CONCRETE SLABS UNDER IMPACT LOADING," *Transactions of the SMiRT 21*, 6-11 November, New Delhi, India
- Schneeberger C., Borgerhoff M., Stangenberg F., Zinn R. (2014) "Analysis of vibration propagation and damping tests of reinforced concrete structures within IMPACT III Project," *Proc. of the 9th Int. Conf. on Structural Dynamics*, EURO DYN 2014, Porto, Portugal, 30 June - 2 July.
- Sugano T., Tsubota H., Kasai Y., Koshika N., Orui S., von Rieseman W.A., Bickel D.C. and Parks M.B., (1993). "Full-scale aircraft impact test for evaluation of impact force," *Nuclear Eng. and Design*, Vol 140, 1993, 373-385.
- Vepsä A. et al. (2011). "IRIS\_2010 - PART II: EXPERIMENTAL DATA," *Transactions of the SMiRT 21*, 6-11 November, 2011, New Delhi, India, Div-V: Paper ID# 520.